MAGNETIC PROPERTIES OF ANTARCTIC STONY METEORITES YAMATO-74115 (H5), -74190 (L6), -74354 (L6), -74362 (L6) AND -74646 (LL6)

Takesi NAGATA and Minoru FUNAKI

National Institute of Polar Research, 9–10, Kaga 1-chome, Itabashi-ku, Tokyo 173

Abstract: The thermomagnetic analysis of five Antarctic chondrites (Yamato-74115 (H5), -74190 (L6), -74354 (L6), -74362 (L6) and -74646 (LL6)) to determine the chemical composition of their metallic components are carried out, together with their magnetic analysis based on the magnetic hysteresis curves at room temperature, for the purpose of a comparison with the results of optical and microprobe analysis of the same chondrites performed by NAGAHARA (Mem. Natl Inst. Polar Res., Spec. Issue, **15**, 77, 111, 1979).

In the Ni-content distribution spectrum in metals obtained by the magnetic analyses (magnetic spectrum), the metallic component consists of α-phase (kamacite) and $(\alpha+\gamma)$-phase (plessite) in Yamato-74115, -74354 and -74646, while it consists of α-, $(\alpha+\gamma)$- and γ-phases in Yamato-74190 and of α-, α_2- and $(\alpha+\gamma)$-phases in Yamato-74362.

In the occurrence frequency spectrum of average Ni-content in individual metallic grains obtained by the microprobe analysis (microprobe spectrum), it is shown that both α- and $(\alpha+\gamma)$- or γ-phases are contained in a number of individual single metallic grains in Yamato-74115, -74354 and -74362. No α-phase is detected in the microprobe spectra of Yamato-74190 and -74646, whereas the major phase of metal in Yamato-74190 is the α-phase of 7 wt% Ni and Yamato-74646 also contains a small amount of α-phase in the magnetic spectra.

The agreement and disagreement between the two kinds of spectrum can give rise to an overall view of both chemical composition and structure of metallic component in the chondrites.

1. Introduction

The mode of occurrence, compositional zoning and bulk chemical composition of metals of Yamato-74115 (H5), -74190 (L6), -74354 (L6), -74362 (L6) and -74646 (LL6) chondrites have been petrologically studied by NAGAHARA (1979b), together with the petrological studies on silicate minerals in these five chondrites (NAGAHARA, 1979a). According to her results, metallic grains in these chondrites are discrete taenite and kamacite, and composite grains of the two phases including plessite. In particular, she constructed the frequency distribution histograms of bulk content of Ni in a large number of individual metallic grains of Yamato-74115, -74354 and

-74362 and further similar histograms for Yamato-74190 and -74646 on the basis of observed data of smaller numbers of metallic grains. For example, the histogram for Yamato-74115 chondrite shows two distinct peaks, one at the kamacite composition and the other at the taenite composition.

It has been pointed out (NAGATA and SUGIURA, 1976; NAGATA, 1978, 1979a, b, c, 1980a), on the other hand, that abundances of kamacite-, taenite-, and plessite-phases in stony meteorites can be reasonably well evaluated by their thermomagnetic analysis on the basis of their magnetic transition temperatures as well as their spontaneous magnetization.

Consonant studies of metallic grains in lunar rocks with the magnetic analyses based on the thermomagnetic characteristics and with the petrological studies with aid of the electron microprobe and optical analyses have been carried out with reasonable success (*e.g.* NAGATA, 1980b), but such consonant studies of metallic grains in chondrites have not yet been reported. In the present study, therefore, these five Yamato chondrites are newly analyzed with the aid of the standard method of magnetic analysis which has been almost established through the magnetic studies on lunar materials and stony meteorites, and the results of magnetic analyses will be compared with the petrological results obtained by NAGAHARA.

2. Basic Magnetic Properties

The basic magnetic parameters at room temperature such as the saturation magnetization (I_s), the saturated IRM (I_R), the coercive force (H_C) and the remanence coercive force (H_{RC}) of the five examined chondrites are summarized in Table 1. Comparatively large values of H_{RC} and H_C of Yamato-74354 and Yamato-74362 chondrites suggest that the martensitic fine structures of plessite phase are abundant in the metallic grains in these chondrites.

Two specimens for each of Yamato-74190 and Yamato-74646 chondrites have been magnetically analyzed in the present work, because an apparent disagreement between the magnetic and the microprobe analyses looks considerably large in Yamato-74190, while Yamato-74646 is a little inhomogeneous LL chondrite. As shown in Table 1, a difference less than factor 2 in magnitude is observed in each of the four magnetic parameters between the two different specimens extracted from a same chondrite. In the present stage of consonant studies of mineralogical structure and chemical composition of metallic grains in chondrites, therefore, it will have to be considered that individual magnitudes of the observed magnetic parameters are associated with a width of $\pm 50\%$ for their degree of inhomogenuity. It should be recommended that several specimens selected at random from a chondrite block are measured and the average of measured values with an estimate of their dispersion is dealt with in the future study of this kind in more detail.

The thermomagnetic analysis of these chondrites have been performed at least

Table 1. Basic magnetic properties of Yamato-74115, -74190, -74354, -74362 and -74646.

	Yamato -74115 (H5)	Yamato -74190 (L6) (1)	Yamato -74190 (L6) (2)	Yamato -74354 (L6)	Yamato -74362 (L6)	Yamato -74646 (LL6) (1)	Yamato -74646 (LL6) (2)	Unit
I_s	25.3	9.3,	12.6	21.8	9.5	3.2,	4.9	emu/gm
I_R	0.60	0.020,	0.018	0.71	0.36	0.026,	0.053	〃
H_C	26	6,	3	66	84	20,	22	Oe
H_{RC}	89	91,	83	2620	2000	405,	195	〃
$\Theta^*_{\alpha\to\gamma}$	740	733,	731	750	765	740,	800	C
$\Theta^*_{\gamma\to\alpha}$	631	615,	612	644	655	—,	745	〃
$\Theta^*_{\alpha+\gamma\to\gamma}$	542	523,	560	542	535	548,	558	〃
$I_s(\alpha)/I_s$	0.86	0.60,	0.74	0.81	0.72	0.09,	0.19	

Remarks

I_s: Saturation magnetization
I_R: Saturated IRM
H_C: Coercive force
H_{RC}: Remanence coercive force
$\Theta^*_{\alpha\to\gamma}$: $\alpha\to\gamma$ transition temperature
$\Theta^*_{\gamma\to\alpha}$: $\gamma\to\alpha$ transition temperature
$\Theta^*_{\alpha+\gamma\to\gamma}$: $(\alpha+\gamma)\to\gamma$ transition temperature
$I_s(\alpha)/I_s$: Ratio of $I_s(\alpha)$ of kamacite phase to total I_s

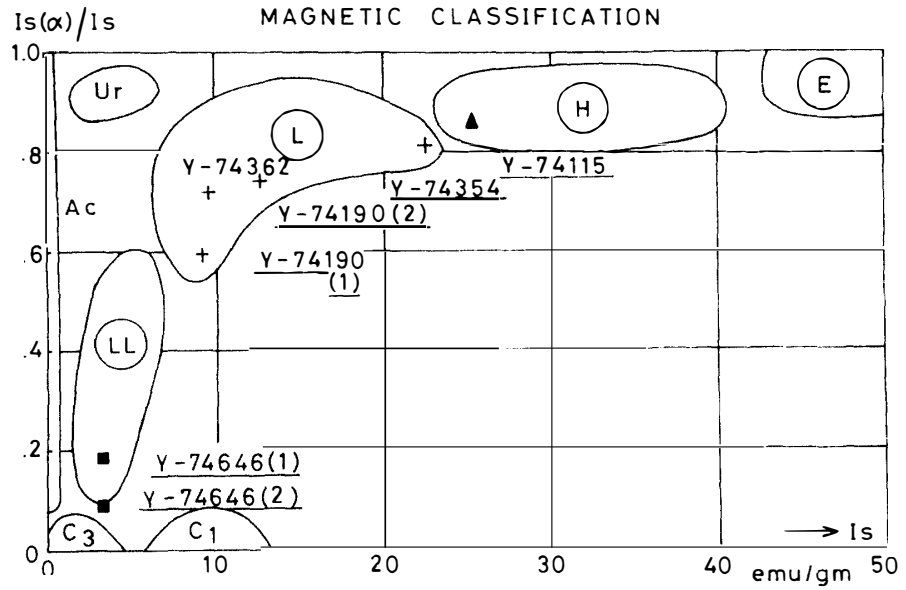

Fig. 1. Plots of I_s and $I_s(\alpha)/I_s$ values of five chondrites under the present study on the $I_s(\alpha)/I_s$ versus I_s diagram for the magnetic classification of stony meteorites.

for the first-run (first heating up to 850°C and then cooling down to 20°C in 10^{-5} Torr vaccum) and then the second-run for each specimen, as discussed later. In Table 1, ratios of the saturation magnetization intensity of kamacite (α-phase) component ($I_s(\alpha)$) to the total saturation magnetization intensity (I_s) for 7 specimens are

summarized. A magnetic classification scheme to chemically classify chondrites (NAGATA, 1979c) and achondrites (1980a) on the basis of magnetically observed values of I_s and $I_s(\alpha)/I_s$ has been proposed with reasonably successful results. In Fig. 1, I_s- and $(I_s(\alpha)/I_s)$-values given in Table 1 are plotted on the proposed $I_s(\alpha)/I_s$ versus I_s diagram for the magnetic classification. As shown in Fig. 1, Yamato-74115 plot is located within the H-chondrite domain, plots of Yamato-74354, Yamato-74362 and 2 specimens of Yamato-74190 within the L-chondrite domain, and plots of 2 specimens of Yamato-74646 are within the LL-chondrite domain. It seems thus that the proposed magnetic classification scheme can be applied on these chondrites too.

3. Thermomagnetic Analysis of Chondrites

The thermomagnetic analysis was carried out in 8×10^{-5} Torr in atmosphere with a Princeton Applied Research vibrating sample magnetometer in a magnetic field of 5 k Oe. In Fig. 2 through Fig. 6, the heating and cooling thermomagnetic curves of the first-run are illustrated (bottom) together with the histogram of average Ni-content of individual metallic grains in the same chondrite sample (top) obtained by NAGAHARA for the five chondrites. In Fig. 3 (Yamato-74190) and Fig. 5 (Yamato-74362), the heating and cooling thermomagnetic curves for the second-run also are superposed in order to demonstrate a difference between the first-run and the second-run heating curves, where their second-run cooling curves are practically identical to the first-run ones.

In the heating processes of these thermomagnetic curves, a non-reproducible magnetic transition at a temperature ($\Theta^*_{\alpha+\gamma\to\gamma}$) between 523°C and 548°C presents the transformation of $(\alpha+\gamma)$-phase (plessite phase) to γ-phase (taenite phase), while a reproducible magnetic transition to completely lose the ferromagnetic magnetization at a temperature ($\Theta^*_{\alpha\to\gamma}$) between 733°C and 765°C presents the reproducible transformation of α-phase (kamacite-phase) to γ-phase. In the cooling thermomagnetic curves, a reproducible magnetic transition at a temperature ($\Theta^*_{\gamma\to\alpha}$) between 615°C and 655°C presents the reproducible transformation of γ-phase to α-phase. In most cases, the γ-phase component as a product of the $(\alpha+\gamma)\to\gamma$ transformation at $\Theta^*_{\alpha+\gamma\to\gamma}$ maintains the γ-phase structure in repeated heating-cooling cycles in the laboratory experiment time-scale. In the case of Fig. 6, for example, the heating and cooling thermomagnetic curves of the second-run are almost identical to the first-run cooling curve, which mostly represents the thermally reversible thermomagnetic curve of an assemblage of taenite phases of various Ni-contents, though a small portion of the I_s-value is due to the presence of a small amount ($I_s(\alpha)/I_s=0.09$) of kamacite phase.

A comparatively steep decrease of I_s with an increase in temperature in the lower temperature range from 0°C to about 200°C in the cooling thermomagnetic curve in

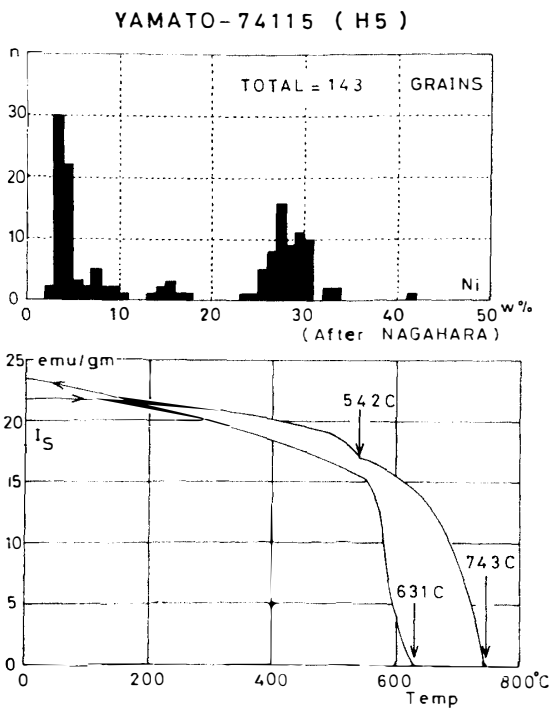

Fig. 2. Occurrence frequency spectrum of average Ni-content in individual metallic grains (top) and the first-run thermomagnetic curves (bottom) of Yamato-74115 (H5).

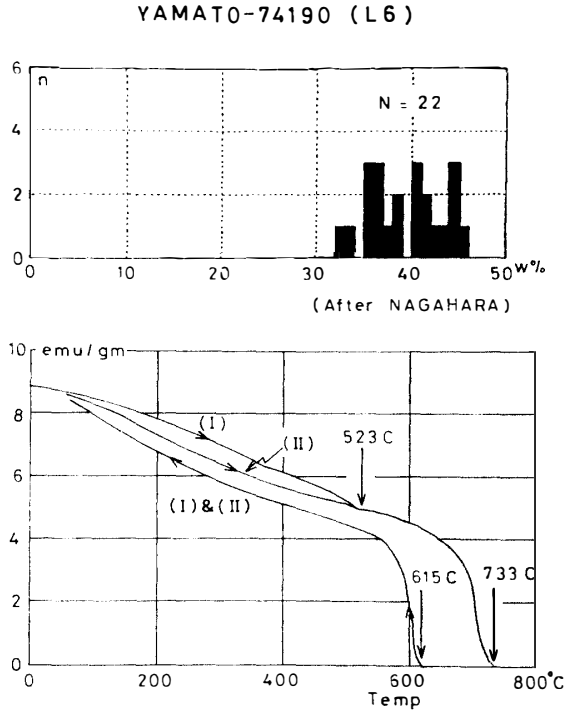

Fig. 3. Occurrence frequency spectrum of average Ni-content in individual metallic grains (top) and the first-run (I) and second-run (II) thermomagnetic curves (bottom) of Yamato-74190 (L6).

Fig. 6 indicates that the distribution spectrum of Ni-content in the taenite phase has a peak (or peaks) of their Curie temperature in the lower temperature range. In the heating thermomagnetic curve of this chondrite also (Fig. 6), a sharp decrease of I_s with temperature just below 548°C suggests that the plessite phase whose $\Theta^*_{\alpha+\gamma\to\gamma}$ temperature is close to 548°C is abundant in the distribution spectrum of average Ni-content in the plessite phases. Since $\Theta^*_{\alpha+\gamma\to\gamma}$ temperature is higher for the plessite phase of smaller Ni-content in the phase equilibrium diagram of Fe-Ni binary system, the apparent value of $\Theta^*_{\alpha+\gamma\to\gamma}$ on the heating thermomagnetic curve ought to present the lower limit of Ni-content in the plessite phases. In the present case, therefore, it can be qualitatively estimated that those FeNi metallic grains are most abundant around a chemical composition of about 30 wt% in Ni-content, of which $\Theta^*_{\alpha+\gamma\to\gamma}$ is about 550°C and Curie temperature for the taenite structure is about 130°C.

The temperature-dependent characteristics of the thermomagnetic curves for the heating and cooling processes in the cases of other chondrites are essentially same as those in the case of Yamato-74646 (Fig. 6). In Fig. 2 (Yamato-74115), for example, the heating thermomagnetic curve of the first-run consists of an $(\alpha+\gamma)$-phase whose

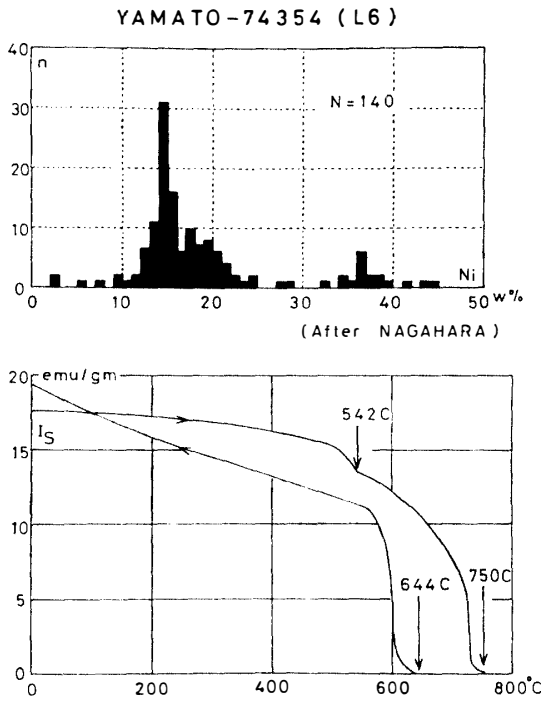

Fig. 4. Occurrence frequency spectrum of average Ni-content in individual metallic grains (top) and the first-run thermomagnetic curves (bottom) of Yamato-74354 (L6).

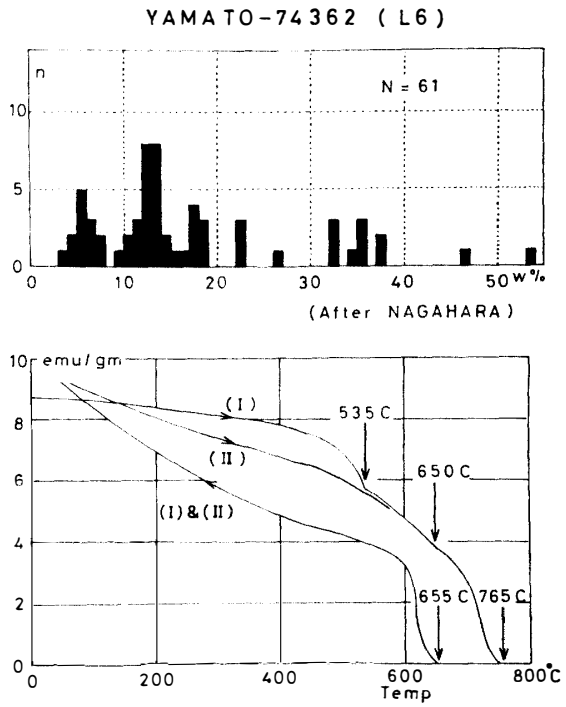

Fig. 5. Occurrence frequency spectrum of average Ni-content in individual metallic grains (top) and first-run and second-run thermomagnetic curves (bottom) of Yamato-74362 (L6).

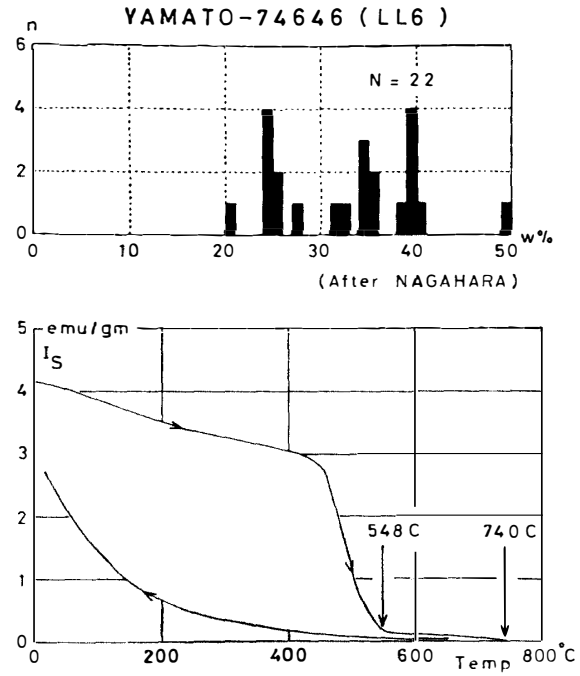

Fig. 6. Occurrence frequency spectrum of average Ni-content in individual metallic grains (top) and the first-run thermomagnetic curves (bottom) of Yamato-74646 (LL6).

representative value of $\Theta^*_{\alpha+\gamma\to\gamma}$ is 542°C and an α-phase whose $\Theta^*_{\alpha\to\gamma}$ is 743°C, while the cooling thermomagnetic curve consists of α-phase whose $\Theta^*_{\gamma\to\alpha}$ is 631°C and a γ-phase whose Curie point extends over a wide temperature range from 0°C to about 550°C. In the second-run thermomagnetic curves, the temperature-dependent characteristics of the α-phase remain as they are in the first-run, whereas those of the γ-phase in the cooling curve of the first-run is practically reproducible in both heating and cooling processes.

In the followings, the observed thermomagnetic curves of individual chondrites will be briefly interpreted in comparison with the distribution spectra of average Ni-contnet in metallic grains observed by NAGAHARA.

3.1. Yamato-74115 (H5) (Fig. 2)

Originally, the group of metallic grains in this H5 chondrite consists of the major component of α-phase whose representative $\Theta^*_{\alpha\to\gamma}$ and $\Theta^*_{\gamma\to\alpha}$ values are 743°C and 631°C respectively, and the minor component of $(\alpha+\gamma)$-phase whose representative $\Theta^*_{\alpha+\gamma\to\gamma}$ is 542°C. A "representative" value for $\Theta^*_{\alpha\to\gamma}$, $\Theta^*_{\gamma\to\alpha}$ and $\Theta^*_{\alpha+\gamma\to\gamma}$ is defined here as a sharp upper limit with respect to temperature for respective transitions. It must be taken into consideration, therefore, that a representative value represents a group of a number of individual elements which gather around the representative value. From each of the observed values of $\Theta^*_{\alpha\to\gamma}$ and $\Theta^*_{\gamma\to\alpha}$, the Ni-content in the α-phase metal can be determined (*e.g.* NAGATA *et al.*, 1973, 1974), where the dependence of $\Theta^*_{\gamma\to\alpha}$ on Ni-content is much more sensitive than that of $\Theta^*_{\alpha\to\gamma}$. In the case of this chondrite, $\Theta^*_{\gamma\to\alpha}$ gives 5.1 wt%, whereas $\Theta^*_{\alpha\to\gamma}$ gives 6.8 wt% Ni. As shown in the bottom of Fig. 2, the saturation magnetization of this α-phase, $I_s(\alpha)$, occupies about 86% of the total saturation magnetization (I_s).

$\Theta^*_{\alpha+\gamma\to\gamma}=542$°C indicated in the figure gives the lower limit (about 26 wt%) of Ni-content in the $(\alpha+\gamma)$-phase, the saturation magnetization of which, $I_s(\alpha+\gamma)$, shares about 14% of I_s. As the cooling thermomagnetic curve indicates, a γ-phase component produced by an irreversible transformation of the $(\alpha+\gamma)$-phase to the γ-phase by heating appears to have a broad distribution of Curie temperature over a temperature range from about 550°C (Curie temperature of 52 wt% Ni γ-phase) to 0°C (Curie temperature of 27 wt% Ni γ-phase).

The thermomagnetic analysis of Yamato-74115 thus gives rise to a qualitative conclusion that the metallic component in this chondrite comprises two distinctly separated groups; a kamacite group of 5–6 wt% Ni which occupies 86% of magnetization (85% in weight) and the other group of plessite of 26–52 wt% Ni which occupies 15% of the total metal weight. The histogram of average Ni-content in 143 metallic grains given in the top of Fig. 2 shows that the metallic grains can be classified into two distinct groups, *i.e.* the kamacite composition (3–8 wt% Ni) and the taenite composition (26–31 wt% Ni). According to NAGAHARA (1979b), a small peak in the range of 13–18 wt% Ni indicates the co-existence of the two compositions

in single grains. Roughly speaking, the result of magnetic analysis is in approximate agreement with the statistical result of the microprobe analysis, at least in identifying the two distinct groups of metal of different chemical compositions.

3.2. Yamato-74190 (L6) (Fig. 3)

As indicated by the heating thermomagnetic curve of the first-run (I) in the figure, the initial composition of the ferromagnetic metallic component of this chondrite comprises ($\alpha+\gamma$)- and γ-phases as well as an α-phase. In the heating thermomagnetic curve of the second-run (II), the ($\alpha+\gamma$)-phase has already been transformed to a γ-phase. $\Theta^*_{\gamma\to\alpha}$ (615°C) and $\Theta^*_{\alpha\to\gamma}$ (733°C) of the α-phase indicates that the Ni-content in the kamacite phase is 6.6 wt%, while $\Theta^*_{\alpha+\gamma\to\gamma}$ (523°C) indicates that the lower limit of Ni-content in the ($\alpha+\gamma$)-phase is 28.3 wt%. It appears that the Ni-content of γ-phase is distributed over a temperature range from about 100°C to 500°C in terms of its Curie temperature (namely, 30–49 wt% in Ni-content). At room temperature, the mutual ratios of saturation magnetization among α-, ($\alpha+\gamma$)-, and γ-phase magnetizations are $I_s(\alpha)$: $I_s(\alpha+\gamma)$: $I_s(\gamma)$=60 : 7: 33 in the result of magnetic analysis.

In the histogram of Ni-content of individual metallic grains shown in the top of Fig. 3, however, no α-phase metal is present, all detected metallic grains containing more than 31 wt% of Ni. Since there might be a possibility that the magnetically examined specimen is a special part of this chondrite by an accidental selection, another piece of Yamato-74190 chondrite is magnetically analyzed. The basic magnetic properties of this second sample, Yamato-74190 (2), are given in Table 1, and its thermomagnetic curves of the first-run is illustrated in Fig. 7 together with those of Yamato-74190 (1) for comparison. The thermomagnetic curves of Yamato-74190 (2) indicate that the metallic component in this sample consists of about 70 wt% of α-phase of 6.7 wt% Ni and 30 wt% of γ-phase in terms of the saturation magnetiza-

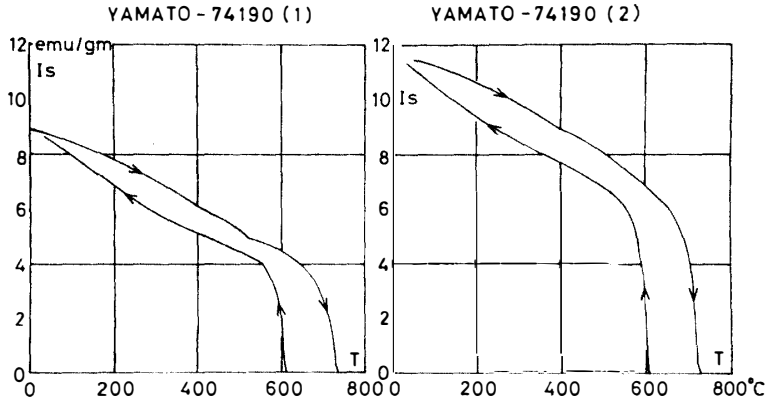

Fig. 7. Comparison of thermomagnetic curves of 2 different specimens, (1) and (2), of Yamato-74190 (L6).

tion intensity. It may be concluded from the present magnetic analysis that the metallic component of Yamato-74190 chondrite consists of a kamacite phase of 6–7 wt% Ni, which occupies about 60–70% of the total magnetization, and the remaining parts of plessite+taenite phase. The observed discrepancy between the magnetic and the microprobe analyses will be discussed in more detail in the later section.

3.3. Yamato-74354 (L6) (Fig. 4)

The thermomagnetic curves of this chondrite consist of a distinct α-phase ($\Theta^*_{\alpha\to\gamma}=$ 750°C, $\Theta^*_{\gamma\to\alpha}=644$°C) and an ($\alpha+\gamma$)-phase ($\Theta^*_{\alpha+\gamma\to\gamma}=542$°C) which is transformed to a γ-phase by the initial heating. Comparing the magnetic analysis data with the result of microprobe analysis, some qualitative agreement between the two results can be observed; namely, the metallic component in this chondrite consists of the major group of Ni-poor FeNi metals and the minor group of Ni-rich (30 wt% Ni) FeNi metals. It is certain in the magnetic data, however, that the major kamacite phase contains 5–8 wt% Ni, whereas the microprobe analysis data show the peak of the occurrence frequency around 13–15 wt% Ni.

3.4. Yamato-74362 (L6) (Fig. 5)

The heating thermomagnetic curve of the first-run of Yamato-74362 is a little complicated, because it has a magnetic transition temperature at 650°C in addition to $\Theta^*_{\alpha+\gamma\to\gamma}=535$°C and $\Theta^*_{\alpha\to\gamma}=765$°C. As shown in Fig. 5, a magnetic phase represented by the transition at 650°C remains in the heating thermomagnetic curve of the second-run, while the plessite phase represented by $\Theta^*_{\alpha+\gamma\to\gamma}=535$°C has been transformed to the taenite phase in the heating thermomagnetic curve of the second-run and in the cooling thermomagnetic curves of the first- and second-runs.

In results of NAGAHARA's microprobe analyses (1979b), an example of metallic grain containing a comparatively large zone (10^2 μm in linear dimension) of about 15 wt% in Ni-content has been pointed out. It seems likely, then, that some portions of metallic grains in this chondrite are of the structure of α_2-phase. Then, the thermomagnetic curves shown in Fig. 4 may be interpreted as composed of an α-phase of 3–6 wt% Ni, an ($\alpha+\gamma$)-phase of larger than 28 wt% in Ni-content and an α_2-phase of 9–24 wt% Ni, where $I_s(\alpha)$: $I_s(\alpha+\gamma)$: $I_s(\alpha_2)$ at room temperature are approximately estimated to be 53: 18: 29.

In the occurrence frequency spectrum of average Ni-content of individual metallic grains in the top of Fig. 5, they can be roughly classified into a kamacite group of 3–8 wt% Ni, a plessite or α_2 group of 9–24 wt% Ni and a taenite group of larger than 32 wt% in Ni-content. In the magnetic analysis, the Ni-rich metallic group is considered to be mostly of plessite structures. However, the two analyses appear to give, in general, the same conclusion that the metallic component in this chondrite comprises the three main groups, *i.e.* a Ni-poor group (3–7 wt% Ni), a Ni-rich group (>30 wt% Ni) and an intermediate Ni group (9–24 wt% Ni), where the Ni-poor kamacite phase is the most abundant.

3.5. Yamato-74646 (LL6) (Fig. 6)

As already discussed, the heating thermomagnetic curve of the first-run of Yamato-74646 is composed of an $(\alpha+\gamma)$-phase of $\Theta^*_{\alpha+\gamma\to\gamma}=548°C$ (Ni-content=26 wt%) and a very small portion of α-phase of $\Theta^*_{\alpha\to\gamma}=740°C$, while the cooling thermomagnetic curve is occupied mostly by the transformed γ-phase, the α-phase magnetization being so small that $\Theta^*_{\gamma\to\alpha}$ is not detectable. The $I_s(\gamma)$ cooling curve indicates that the Ni-content in the transformed γ-phase is distributed from 27 to 52 wt%.

In the occurrence frequency spectrum of average Ni-content also, almost all metallic grains contain more than 25 wt% of Ni. Thus, the magnetic analysis has resulted in a qualitatively same conclusion on the chemical composition of metallic component in this chondrite as the result of the microprobe analysis. As the Ni-rich taenite grains were observed by NAGAHARA (1979b) in this chondrite, another specimen of this chondrite, Yamato-74646 (2), is magnetically analyzed. The thermomagnetic curves of the first-run of Yamato-74646 (2) are shown in Fig. 8 in comparison with those of Yamato-74646 (1). The heating thermomagnetic curve of Yamato-74646 (2) looks apparently much different from that of Yamato-74646 (1), the former comprising an abundant group of γ-phase and small amounts of $(\alpha+\gamma)$-phase ($\Theta^*_{\alpha+\gamma\to\gamma}=558°C$) and α-phase ($\Theta=805°C$), where $I_s(\alpha):I_s(\alpha+\gamma):I_s(\gamma)=19:7:74$. The thermomagnetic curves of the second-run of Yamato-74646 (2) and its cooling thermomagnetic curve of the first-run are simply composed of an α-phase ($\Theta^*_{\gamma\to\alpha}=748°C$) of $I_s(\alpha)/I_s=0.19$ and a γ-phase of $I_s(\gamma)/I_s=0.81$, where the taenite magnetization of lower Curie temperature (*i.e.* poorer content of Ni) is stronger. It may be concluded thus that taenite or plessite phase rich in Ni (>25 wt%) occupies more than 80% of the metallic component in this chondrite Yamato-74646.

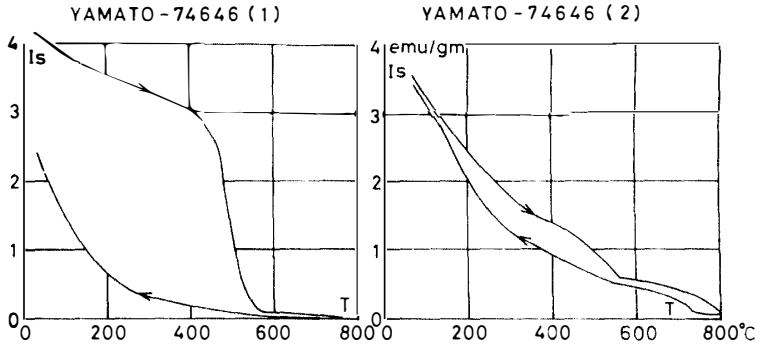

Fig. 8. Comparison of thermomagnetic curves of 2 different specimens, (1) and (2), of Yamato-74646 (LL6).

4. Semi-Quantitative Magnetic Analysis of Stony Meteorites

The saturation magnetization $I_s(T)$ at temperature (T) of an assemblage of ferromagnetic grains which consists of a large number of individual magnetic phases

of Θ in the Curie temperature, $I_s(\Theta, T)$ in the saturation magnetization at T and $f(\Theta)$ in the density of distribution can be expressed by

$$I_s(T)=\int_0^{\Theta_m} I_s(\Theta, T)f(\Theta)d\Theta\,, \tag{1}$$

where Θ_m denotes the maximum Curie temperature. The elementary data necessary to deal with eq. (1) are the basic characteristics of $I_s(\Theta, T)$ dependent on T for various Ni-contents (from 0 to 100% Ni) of FeNi alloys, and if possible, of Fe-Ni-Co-P alloys for 0–3 wt% of Co and 0–2 wt% of P. Unfortunately, however, comprehensive experimental data for such a purpose as mentioned above have not yet been completely obtained. At the present stage, the magnetic data of FeNi alloys summarized by HOSELITZ and SUCKSMITH (1943), BOZORTH (1951), and CRANGLE and HALLAM (1963) can be referred as the basic characteristics of $I_s(\Theta, T)$ of α-, α_2- and γ-phases. As for the unequilibrated $(\alpha+\gamma)$-phase, it seems that the magnetic analysis to determine the Ni-content spectrum is almost impossible, except for the determination of the lower limit of Ni-content from $\Theta^*_{\alpha+\gamma\to\gamma}$, whence the Ni-content of this phase is determined on the transformed γ-phase after a sufficient heating procedure. When an $(\alpha+\gamma)$-phase coexists with a γ-phase, the γ-phase magnetization component in the first-run heating thermomagnetic curve is first analyzed to determine the Ni-content spectrum, and then the magnetization component of the original γ-phase plus the newly produced γ-phase by the transformation from the $(\alpha+\gamma)$-phase in the first-run or second-run cooling thermomagnetic curve or the second-run heating thermomagnetic curve is analyzed to determine the total Ni-content spectrum of the original γ-phase plus the original $(\alpha+\gamma)$-phase. Thus, the Ni-content spectrum of the $(\alpha+\gamma)$-phase is determined as their difference.

From observed values of $I_s(T)$ and the given curve of $I_s(\Theta, T)$, the distribution function $f(\Theta)$ can be obtained by numerically solving the integral equation expressed by eq. (1). As Θ and $I_s(\Theta, T)$ are single-value functions of the Ni-content in both the α- and γ-phases, the occurrence frequency spectrum in weight of the metallic component of Ni in Ni-content, M(Ni), is directly given from $f(\Theta)$. In Fig. 9 through Fig. 13, the Ni-content spectra of the five chondrites thus estimated are shown in comparison with respective spectra of the average Ni-content of individual metallic grains observed by NAGAHARA, where M(Ni) in the bottom diagrams is expressed by the weight per cent in respective chondrites for each 1% intervals of Ni-content.

As already discussed in the preceding section, no exact agreement can be observed between the Ni-content spectrum obtained by the magnetic analysis (magnetic spectrum) and that obtained by the microprobe analysis (microprobe spectrum). In her paper (NAGAHARA, 1979b), NAGAHARA stated (a) that if a grain contains both kamacite and taenite, the bulk composition of Ni should be more than that of kamacite only, and if an isolated kamacite exists, the bulk composition of the grain should be below 7 wt% Ni; so that the small peak in the range of Ni 13–18 wt% (in the top diagram of

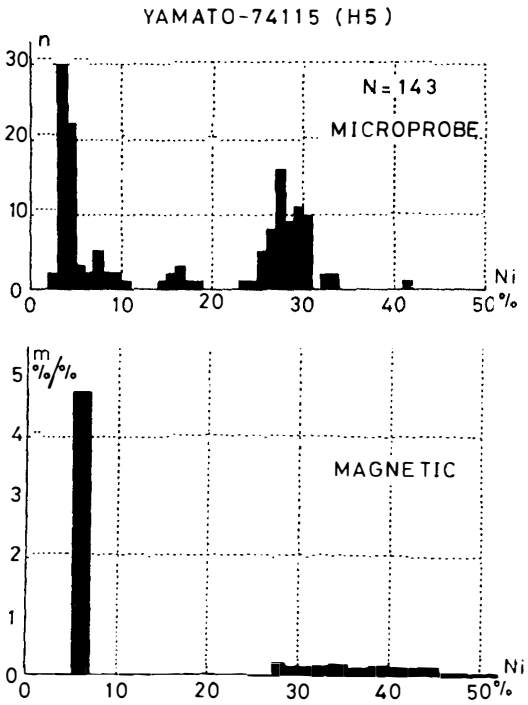

Fig. 9. Comparison of magnetic spectrum with microprobe spectrum for Ni-content in metals of Yamato-74115.

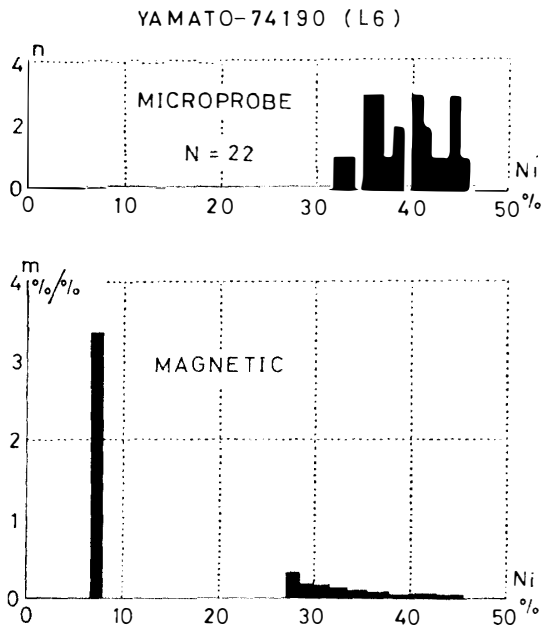

Fig. 10. Comparison of magnetic spectrum with microprobe spectrum for Ni-content in metals of Yamato-74190.

Fig. 9) indicates the association of the two phases (α- and γ-phases) in a single grain, and (b) that all metal grains in Yamato-74190 (Fig. 10) and Yamato-74646 (Fig. 13) are high-Ni taenite; however, it is not certain whether no kamacite grains exist, because of the scarcity of analyzed grains.

Statement (a) for the microprobe spectrum can be considered as one of the main causes for the observed difference between the magnetic and microprobe spectra, because the magnetic spectrum presents the integrated distribution spectrum of Ni-contents of ferromagnetic metallic phases regardless of their structure and size. If both the magnetic and microprobe spectra are fully accurate, a combination of the two spectra can give rise to an interpretation of the composition and structure of metallic phases in some more detail. In the case of Yamato-74115 in Fig. 9, for example, the microprobe spectrum can be interpreted in such a way that metallic grains composing the second large peak of 26–31 wt% Ni are composed of kamacite phase and taenite phase of larger than 28 wt% in Ni-content and grains of the small peak of 13–18 wt% Ni are combinations of kamacite and taenite as described by NAGAHARA.

The conspicuous peak of 13–22 wt% Ni in the microprobe spectrum of Yamato-74354 (Fig. 11) also may be composed of metallic grains which comprise the kamacite of 6–8 wt% Ni and the taenite of larger than 27 wt% in Ni-content given by the magnetic spectrum. The magnetic spectrum of Yamato-74362 (Fig. 12) is in compara-

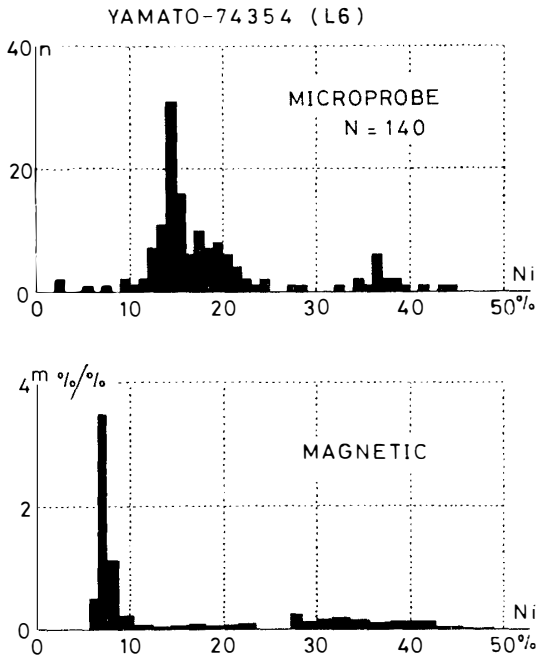

Fig. 11. Comparison of magnetic spectrum with microprobe spectrum for Ni-content in metals of Yamato-74354.

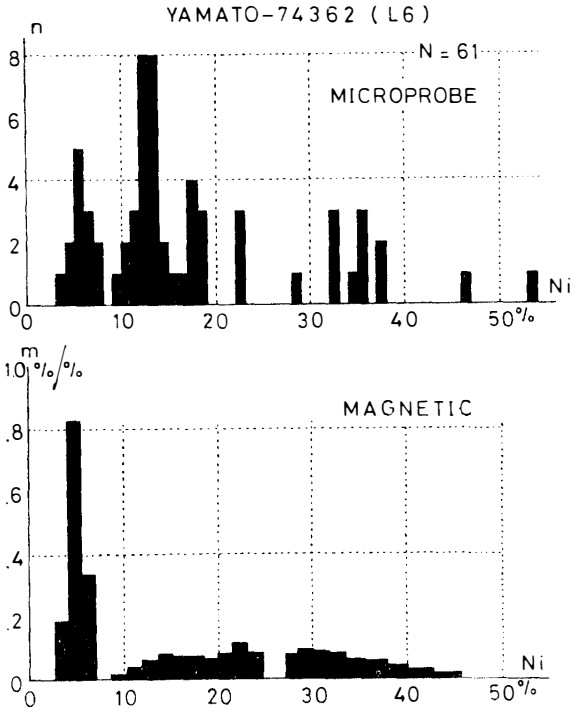

Fig. 12. Comparison of magnetic spectrum with microprobe spectrum for Ni-content in metals of Yamato-74362.

tively good agreement with the microprobe spectrum. Namely, both spectra consist of a kamacite group of 4–8 wt% Ni, an α_2-phase group of 9–23 wt% Ni and a taenite group larger than 28 wt% in Ni-content. If the largest peak of 12–15 wt% Ni in the microprobe spectrum is interpreted as an combination of the kamacite phase and the α_2- or taenite phase in individual metallic grains, both spectra can be considered reasonably consistent.

As for Yamato-74646 (in Fig. 13), the major characteristic of the microprobe spectrum that all metallic grains are in γ-phase or Ni-rich $(\alpha+\gamma)$-phase (larger than 20 wt% in Ni-content) is in agreement with the composition of the magnetic spectrum which consists of the absolutely large group of γ-phase or Ni-rich $(\alpha+\gamma)$-phase larger than 28 wt% in Ni-content and a very small group of kamacite phase of about 6 wt% Ni. As suggested by the statement (b) of NAGAHARA, there is a possibility that the presence of kamacite phase in this chondrite may have been overlooked in the microprobe spectrum because the total number of measured metallic grains is not sufficiently large for detecting the small abundance of kamacite phase (*i.e.* $I_s(\alpha)/I_s=0.09$–0.19 in Table 1).

As for Yamato-74190 chondrite (Fig. 10), however, no kamacite phase is present in the microprobe spectrum, whereas a kamacite group of about 7 wt% Ni is more

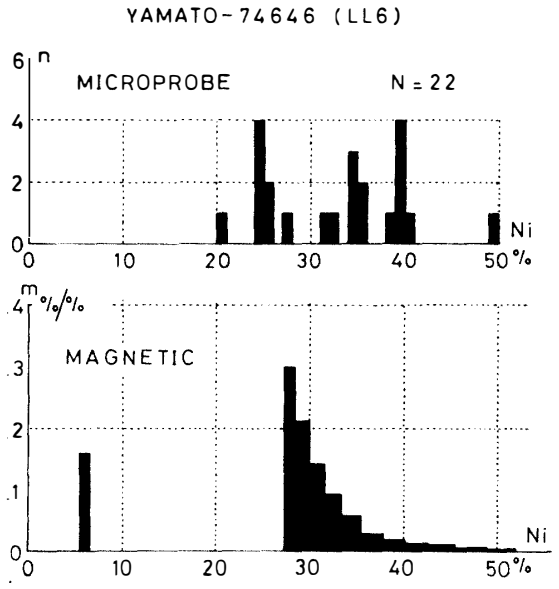

Fig. 13. Comparison of magnetic spectrum with microprobe spectrum for Ni-content in metals of Yamato-74646.

abundant ($I_s(\alpha)/I_s$=0.60–0.74 in Table 1) than a Ni-rich metallic group of taenite and plessite in the magnetic spectrum. As shown in Fig. 7, the abundant presence of the kamacite phase is definitely detected in the thermomagnetic curves of two different specimens of Yamato-74190 chondrite. If some comparatively large metallic grains in this chondrite are occupied mostly by kamacite-phase, it may be statistically unlikely that they are missed in the microprobe observations of 22 individual grains. Then, the most plausible interpretation of the considerable difference between the magnetic and microprobe spectra would be to assume that the majority of kamacite metal are in the form of very fine grains which are too small to be analyzed by the microprobe. A feasibility of this interpretation could be supported by the observed fact that H_C and I_R/I_s of Yamato-74190 are abnormally smaller than those of the other H- and L-chondrites (Table 1). As already discussed in the case of lunar rocks (NAGATA *et al.*, 1972), the coexistence of superparamagnetically fine grains together with a ferromagnetic component gives rise to a considerable decrease in the apparent value of H_C. Since I_R=0 for the superparamagnetically fine grains, the observed value of I_R presents the saturated IRM of the ferromagnetic component only. If the relative abundance of the superparamagnetically fine grains becomes larger, therefore. both H_C and I_R/I_s become smaller, approaching to zero at the extreme case that the whole ferromagnetic metals completely consist of the superparamagnetic component only. Thus, the observed apparent absence of kamacite phase in the microprobe spectrum and the abnormally small values of H_C and I_R/I_s of Yamato-74190 chondrite could be consistently interpreted, at least qualitatively.

It must be noted, however, that the presence of kamacite grains in Yamato-74190 has been reported by KIMURA *et al.* (1978). Then, the apparent absence of kamacite

phase in the microprobe spectrum may be partly due to the scanty number of observed metallic grains, as suggested by NAGAHARA, and partly due to the superparamagnetically fine grain size of the major parts of kamacite phase.

5. Concluding Remarks

The main aim of both the petrological studies with the aid of optical microscopes and a microprobe by NAGAHARA and the present magnetic studies is the determination of chemical composition and structure of metallic components in the chondrites which can give information of their thermal history in the past.

Metallographical studies to deal with the thermal history of meteorites have been extensively carried out mostly with iron meteorites (*e.g.* WOOD, 1964; GOLDSTEIN and OGILVIE, 1965; GOLDSTEIN and SHORT, 1967a, b). The most fundamental factor in theoretically discussing the thermal history of meteoritic FeNi metals will be the diffusion coefficients for Ni atoms through the bcc crystal lattice of α-phase and the fcc crystal lattice of γ-phase as a function of temperature and Ni-content. Since it has been experimentally ascertained that the diffusion coefficient (D_α) through α-phase is more than 10^2 as large as that through γ-phase (D_γ) (GOLDSTEIN *et al.*, 1964), D_α/D_γ can be considered infinitely large in an approximate discussion (GOLDSTEIN and OGILVIE, 1965). The magnitude of D_γ dependent on temperature (T) and Ni-content (C_{Ni}) is given by GOLDSTEIN *et al.* (1964) as

$$D_\gamma = \exp(0.0519 C_{\mathrm{Ni}} + 1.15) \exp\left\{-\frac{76400 - 11.6 C_{\mathrm{Ni}}}{RT}\right\}, \tag{2}$$

where C_{Ni} is given in atomic per cent. Namely, D_γ decreases exponentially with a decrease of T, and D_γ at a certain temperature is larger for a Ni-richer taenite. In the case of octahedrite iron meteorites, it has been reported (*e.g.* WOOD, 1964; GOLDSTEIN and OGILVIE, 1965) that their cooling rate during a temperature range between 600 to 400°C is estimated to be 1–10 degrees per million years. These research works are mostly concerned with the Widmanstätten structure of the octahedrites, in which each structure of α- and γ-phases is visually large.

The thermal history of chondrites may have to be considerably different from that of iron meteorites, which are assumed to be originally located near the center of hypothetical parent planets, because the chondrites could be parts of a planetesimal whose diameter is much smaller than that of a primordial planet which has a metallic core, and further there may be no evidence to assume that individual metallic grains have come from the same single phase metal which is in the γ-phase at high temperatures above 800°C. For example, the Ni-rich phase in all the present five chondrites are mostly in the $(\alpha+\gamma)$-phase, which has $\Theta^*_{\alpha+\gamma\to\gamma}$ in a narrow temperature range of 523–548°C, as shown in Figs. 2 through 6, regardless of the average Ni-content in the bulk chemical composition, and the $(\alpha+\gamma)$-phase is transformed to the γ-phase only by once heating beyond the critical $\Theta^*_{\alpha+\gamma\to\gamma}$ temperature. This magnetically

observed fact suggests that these chondrites were cooled sufficiently slowly to keep the phase equilibrium down to about 550°C, and then the cooling rate below about 550°C was not slow enough to differentiate into the discrete α- and γ-phases, except Yamato-74190 which contains both $(\alpha+\gamma)$- and γ-phases in the original state.

An interesting magnetically observed fact is concerned with Yamato-74646 (LL6) chondrite. In the original state, the metallic component of Yamato-74646 (1) consists of mostly an $(\alpha+\gamma)$-phase and a very small portion of α-phase, while that of Yamato-74646 (2) consists of mostly a γ-phase and small portions of α- and $(\alpha+\gamma)$-phases (Fig. 8). In both specimens, the chemical composition of metal is represented by about 30 wt% Ni, but the differentiation into α- and γ-phases in the cooling process advanced in Yamato-74646 (2) much more than in Yamato-74646 (1) in the same piece of this chondrite. In other words, the differentiation of an $(\alpha+\gamma)$-phase into α- and γ-phases can be sensitively examined on the thermomagnetic curves Since many other chondrites are characterized by the presence of an $(\alpha+\gamma)$-phase of $\Theta^*_{\alpha+\gamma\to\gamma}\simeq 550$°C (*e.g.* NAGATA, 1979a, c), this problem will be discussed in more detail elsewhere.

Another interesting magnetically observed fact may be the presence of an α_2-phase in Yamato-74362. Briefly summarizing, it will be almost certain that this chondrite was shock metamorphazed, resulting in a partial remelting of metallic component followed by a rapid cooling.

By comparing the magnetic spectra of metallic component with the microprobe spectra for chondrites, it seems that both agreement and disagreement between them suggest a possibility to establish a consonant study method to deal with much more detail of the composition and structure of metallic component in chondrites and resulting possible interpretations of the thermal history of chondrites.

References

BOZORTH, R. M. (1951): Ferromagnetism. New York, Van Nostrand, 968 p.

CRANGLE, J. and HALLMAN, G. C. (1963): The magnetization of face-centered cubic and body-centered cubic iron+nickel alloys. Proc. R. Soc. London, Ser. A, **272**, 119–132.

GOLDSTEIN, J. I., HANNEMAN, R. E. and OGILVIE, R. E. (1964): Diffusion in the Fe-Ni system at 1 atmosphere and 40 k bars pressure. Trans. Metall. Soc. AIME, **233**, 812–820.

GOLDSTEIN, J. I. and OGILVIE, R. E. (1965): The growth of the Widmanstätten pattern in metallic meteorites. Geochim. Cosmochim. Acta., **29**, 893–920.

GOLDSTEIN, J. I. and SHORT, J. M. (1967a): Cooling rates of 27 iron and stony-iron meteorites. Geochim. Cosmochim. Acta., **31**, 1001–1023.

GOLDSTEIN, J. I. and SHORT, J. M. (1967b): The iron meteorites, their thermal history and parent bodies. Geochim. Cosmochim. Acta., **31**, 1733–1770.

HOSELITZ, K. and SUCKSMITH, W. (1943): A magnetic study of two-phase iron-nickel alloys II. Proc. R. Soc. London, Ser. A, **181**, 303–313.

KIMURA, M., YAGI, K. and OBA, Y. (1978): Petrological studies of Yamato-74 meteorites (2). Mem. Natl Inst. Polar Res., Spec. Issue, **8**, 156–169.

NAGAHARA, H. (1979a): Petrological studies on Yamato-74354, -74190, -74362, -74646 and -74115 chondrites. Mem. Natl Inst. Polar Res., Spec. Issue, **15**, 77–109.

NAGAHARA, H. (1979b): Petrological studies of Ni-Fe metal in some ordinary chondrites. Mem. Natl Inst. Polar Res., Spec. Issue, **15**, 111–122.

NAGATA, T. (1978): Supplementary notes on the magnetic classification of stony meteorites. Mem. Natl Inst. Polar Res., Spec. Issue, **8**, 233–239.

NAGATA, T. (1979a): Magnetic classification of Antarctic meteorites (III). Mem. Natl Inst. Polar Res., Spec. Issue, **12**, 233–237.

NAGATA, T. (1979b): Magnetic properties of Yamato-7301(j), -7305(k) and -7304(m) chondrites in comparison with their mineralogical and chemical compositions. Mem. Natl Inst. Polar Res., Spec. Issue, **12**, 250–269.

NAGATA, T. (1979c): Magnetic classification of stony meteorites (IV). Mem. Natl Inst. Polar Res., Spec. Issue, **15**, 273–279.

NAGATA, T. (1980a): Magnetic classification of Antarctic achondrites. Mem. Natl Inst. Polar Res., Spec. Issue, **17**, 219–232.

NAGATA, T. (1980b): Viscous magnetization and ferromagnetic composition of stony meteorites and lunar materials. Mem. Natl Inst. Polar Res., Spec. Issue, **17**, 243–257.

NAGATA, T., FISHER, R. M. and SCHWERER, F. C. (1972): Lunar rock magnetism. Moon, **4**, 160–186.

NAGATA, T., FISHER, R. M., SCHWERER, F. C., FULLER, M. D. and DUNN, J. R. (1973): Magnetic properties and natural remanent magnetization of Apollo 15 and 16 lunar materials. Proc. Lunar Sci. Conf. 4th, 3019–3043.

NAGATA, T., SUGIURA, N., FISHER, R. M., SCHWERER, F. C., FULLER, M. D. and DUNN, J. R. (1974): Magnetic properties of Apollo 11–17 lunar materials with special reference to meteorite impact. Proc. Lunar Sci. Conf. 5th, 2827–2839.

NAGATA, T. and SUGIURA, N. (1976): Magnetic characteristics of some Yamato meteorites–Magnetic classification of some meteorites. Mem. Natl Inst. Polar Res., Ser. C, **10**, 30–58.

WOOD, J. A. (1964): The cooling rates and parent planets of several iron meteorites. Icarus, **3**, 429–459.

(*Received May 1, 1981*)